Multi-Objective Optimization of Energy Retrofit for Existing Buildings Using an Enhanced Chimp Optimization Algorithm

Hualong Zhang
Zhengzhou Urban Construction Vocational College, Zhengzhou, China
E-mail: hooloong271523429@163.com

Keywords: existing buildings, retrofit, energy consumption, multi-objective optimization, chimp optimization algorithm

Received: February 26, 2025

This study proposes a modified multi-objective chimp optimization algorithm (MO-ChOA) to optimize energy consumption retrofits for existing buildings to reduce operational energy consumption. First, a back-propagation neural network was used to predict carbon emission factors, and a mathematical model for multi-objective optimization of building energy consumption was established. Subsequently, Hammersley sequence and somersault foraging heuristic strategy were introduced to improve MO-ChOA, and the improved MO-ChOA was used to solve the multi-objective optimization model of building energy consumption. The experimental results showed that the proposed improved MO-ChOA had a reverse generation distance of 0.113 and a super volume of 0.973, which was superior to the traditional MO-ChOA. This study proposed a modified MO-ChOA to optimize energy consumption retrofits for existing buildings, aiming to reduce operational energy consumption. First, a back-propagation neural network was used to predict carbon emission factors, and a mathematical model for multi-objective optimization of building energy consumption was established. In the optimization of building energy consumption, the proposed method had a solution interval of only 0.110, an average uniformity evaluation index of more than 0.8, a carbon emission saving rate of 0.7-0.95, a cost saving rate of 0.79, and an investment return rate of 0.685, which could effectively reduce carbon emissions and operating costs. The study encourages the development and innovation of energy-saving retrofitting technologies and offers new technical tools and solutions for retrofitting existing buildings with lower energy use.

Povzetek: Predlagan je izboljšan večciljni metahevristični algoritem optimizacije šimpanzov z Hammersleyjevim vzorčenjem in strategijo, ki učinkovito zmanjša porabo energije ter emisije pri energetski sanaciji stavb.

1 Introduction

The building industry is a major contributor to energy consumption (EC) and CO2 emissions. A large number of old residential buildings have poor envelope structures, old and inefficient equipment, and a large proportion of non-energy efficient buildings. Moreover, the lack of operation and maintenance management leads to a high percentage of building whole-life EC in the total EC [1-2]. In conclusion, achieving carbon peak, carbon neutrality, and advancing green, low-carbon, and high-quality development all depend heavily on accelerating the promotion of energy saving (ES) and carbon reduction (CR) in the building industry. In the meanwhile, building CR initiatives can raise the energy efficiency level of buildings by utilizing ES materials, optimizing building design, and taking other steps. Buildings must conduct ES and CR since this can give occupants a more comfortable and healthful living environment [3]. Building operations contribute significantly to carbon emissions (CEs). Reducing EC directly lowers emissions while improving energy efficiency. Retrofitting existing buildings (EBs) for energy efficiency is still fraught with difficulties, though. On the one hand, the current energy efficiency retrofit schemes are less generalizable due to the complexity of the EB stock and the range of building kinds, ages, and purposes. For example, building types can be divided into residential buildings, public buildings, industrial buildings, and agricultural buildings according to their functions. According to the structural form, it can be divided into wall load-bearing structure, skeleton structure, etc. It also includes special types of buildings such as historical buildings and memorial buildings. On the other hand, the integration of multiple technologies such as renewable energy integration and smart building technologies for the energy efficiency retrofit design of existing EBs increases the complexity of technology implementation [4-5]. Multi-objective optimization algorithm (MOOA) refers to an algorithm that searches for a set of non-inferior solutions in optimization problems where there are conflicts or contradictions among multiple objective functions (OFs). In recent years, MOOA has been widely applied in fields such as engineering design, supply chain management, and logistics optimization due to its unique advantages in handling multiple conflicting

or contradictory OFs. The energy-saving renovation of EBs faces challenges such as complex types and poor universality of schemes. This study aims to optimize the EC and cost of EBs through an improved MOOA to reduce operational EC, reduce CEs, and improve energy use efficiency. The study first determines the CE indexes of EB operations based on the ES objectives and CE factors, and constructs a mathematical multi-objective optimization (MOO) model. Then, the Hammersley sequence and somersault foraging heuristic strategy are introduced to improve the Chimp optimization algorithm (ChOA), which aims to enhance the multi-objective optimization performance of ChOA and achieve energy and cost optimization of EBs.

The study is mainly composed of four sections. The first section reviews the relevant studies on building ES and emission reduction optimization at home and abroad. The second section describes the construction of MOO model for EC of EBs and the design process of the improved multi-objective chimp optimization algorithm (MO-ChOA) solution algorithm. In the third section, the improved MO-ChOA solution algorithm is tested for performance and the EC optimization analysis is carried out. The fourth section summarizes the experimental results.

2 Related work

Renovating buildings contributes to a decrease in EC and CEs, which has broad social and practical implications as well as significant theoretical importance. Research on ES and emission reduction in buildings has been conducted by numerous academics and researchers. To properly analyze the energy performance of buildings, Fallah et al. used feed-forward neural network combined with electrostatic discharge algorithm to optimize and design an annual thermal energy demand prediction model for residential buildings. Experimental results indicated that the method demonstrated higher prediction accuracy compared to atomic search optimization, future search algorithm and satin gardener bird optimization [6]. To control building EC towards sustainable buildings, Tahmasebinia et al. explored the potential of building information modeling (BIM) and digital twin technology in building energy efficiency and management, supported by citing case studies [7]. An energy-efficient building management information system based on multi-intelligent body topology was proposed by Verma et al. to address the conflict between occupant comfort and EC in residential structures. To find the best way to reduce EC and increase comfort, the system first optimized the environmental parameters using a restricted nonlinear optimization algorithm. Artificial intelligence (AI) and deep learning techniques were then used to further train and validate the system. The findings proved that the system successfully decreased EC while maintaining high levels of occupant satisfaction with regard to air quality, thermal comfort, and visual comfort [8]. To optimize the design of commercial buildings in the tropical climate of India to enhance thermal performance and reduce EC, Sana et al. used building energy simulation optimization (BESO) in conjunction with grasshopper optimization algorithm (GOA). The experimental results indicated that the method performed better in reducing the annual thermal load and was more computationally efficient with a reduction in computation time by 4.18%-37.11% [9]. To solve the problems of low efficiency and high cost of traditional building construction and to promote the green and sustainable development of buildings, Wu constructed a multi-objective decomposition building energy efficiency optimization model based on BIM. It also introduced the intelligent body-assisted multi-objective particle swarm optimization (MOPSO) to enhance the optimization effect. According to the experimental findings, the model exhibited good convergence, adaptability, and optimization time performance. In particular, it achieved the shortest search time, the smallest total EC and the highest oversize volume index in the ES optimization design of urban single-room office buildings [10]. Khan et al. proposed a bacterial foraging ant colony optimization algorithm to schedule electricity consumption for building energy optimization problems. The results showed that the proposed algorithm could reduce electricity cost and improve user comfort [11]. Xu et al. proposed a building EC optimization model based on convolutional neural networks and BIM. The results showed that the proposed method could reduce building EC by 24.53% and increase natural lighting by 18.98% [12]. Gheoany et al. proposed an energy management system based on branch and bound algorithm and particle swarm optimization algorithm for building energy management problems. The results showed that the proposed method could reduce the electricity bills and standard number of poles by 28% and 49.32%, respectively [13].

To optimize the building envelope and photovoltaic modules to enhance the performance of energy-efficient buildings, Zhao et al. constructed an efficient hybrid algorithm using PSO, support vector machines, non-dominated sorting genetic algorithms (NSGA) II, and sequential selection of optimization techniques. The method significantly reduced building EC by 41%, CE by 34% and retrofit operation cost by 20% [14]. Building envelopes can be retrofitted to adapt to the future climate using a MOO design process that Ding et al. designed to address the impact of global climate change on building EC. The method utilized back-propagation neural network (BPNN) to establish the correlation between design parameters and performance metrics and NSGA-III to optimize the retrofit strategy. The results revealed that the method was more efficient in terms of ES solutions, emphasizing the importance of considering climate change factors [15]. To address the problem of high dependence on expert knowledge and subjective decision making in traditional green building design, Khan et al. proposed an innovative framework integrating BIM, interpretable AI and MOO. The framework used Bayesian optimization for energy prediction and MOO with the help of multi-objective evolutionary algorithm (MOEA) based on decomposition. The results revealed that the framework achieved highly accurate prediction and significant optimization results, improved energy

efficiency and thermal comfort, and reduced CO_2 emissions [16]. To solve the MOO problem in the renovation of historic buildings, Wei et al. proposed a renovation method that combines the building envelope with systematic standard measures. Using energy simulation technology and NSGA-II algorithm, multiple retrofit solutions were generated by logarithmic additive decomposition, and then the weighted sum method was applied to find the optimal solution. Taking the Nanjing Courtyard as an example, EC was reduced by 63.62% after the retrofit, the net present value increased by 151.84%, and the CR rate was up to 60.48%, which realized the balance of ES, CR and economy [17]. The summary table of the above-mentioned related work is shown in Table 1.

Table 1: Summary table of related work

Literature	Method	Optimization objectives	Performance indicators	Limitation
[6]	Feed-forward neural network, electrostatic discharge algorithm	Forecast of annual thermal energy demand for residential buildings	Prediction accuracy	High dependence on data quality and integrity
[7]	BIM, digital twin technology	Building energy efficiency and management	Energy saving effect and management efficiency	The technical implementation is complex and the initial cost is high
[8]	Multi agent topology, constrained nonlinear optimization, deep learning	Minimizing energy consumption and maximizing living comfort	Satisfaction with energy consumption, thermal comfort, visual comfort, and air quality	The system requires high real-time performance, and there is a significant demand for computing resources during large-scale deployment
[9]	BESO, GOA	Optimization of thermal performance of commercial buildings in tropical climate	Annual heat load, calculation time	Specific to tropical climates, limited generalization ability to other climate types
[10]	BIM, Multi-objective decomposition model and MOPSO	Energy efficiency optimization of urban single room office buildings	Search time, total energy consumption, super large volume index	Sensitive to building types and requiring customized adjustments
[11]	Bacterial foraging ant colony optimization algorithm	Optimization of building electricity dispatch	Electricity cost, user comfort	The algorithm has high complexity and requires frequent parameter adjustments in practical applications
[12]	Convolutional neural networks, BIM	Optimization of building energy consumption and natural lighting	Energy consumption and natural lighting	Relying on large-scale training data, model training takes a long time
[13]	Branch and bound algorithm, PSO	Home energy management	Electricity cost, standard pole count	Insufficient scalability of large-scale residential areas
[14]	PSO, SVM, and NSGA-II	Building envelope structure and optimization of photovoltaic modules	Energy consumption, carbon emissions, and operating costs	High complexity of multi algorithm integration

[15]	BPNN and NSGA-III	Future climate adaptive building envelope renovation	Efficiency	The uncertainty of climate change prediction affects the reliability of optimization results
[16]	BIM, explainable AI and MOEA	Energy performance analysis of green buildings	Energy efficiency, carbon dioxide emissions	Explainable AI implementation is complex, requiring a balance between model accuracy and interpretability
[17]	NSGA-II, logarithmic additive decomposition	Energy saving renovation of historical buildings	Energy consumption, net present value, carbon reduction rate	There are many restrictions on the renovation of historical buildings, which require coordination among multiple stakeholders

In summary, in the area of ES and emission reduction in building retrofitting, which successfully increases building energy efficiency and comfort by adding cutting-edge algorithms and technologies, current research has produced noteworthy outcomes. Nonetheless, the majority of current studies concentrate on optimizing the structure and performance of a particular building.

To reduce the operational EC of EBs, the study innovatively constructs a mathematical MOO model and introduces intelligent optimization algorithms to improve the optimization, in order to achieve further optimization of EC.

3 optimization study of operational energy retrofit in EBS

The study unfolds the optimal design of operational energy retrofit of EBs in the context of carbon peak ES and the MOO study of ES with the help of multi-objective intelligent algorithms.

3.1 Construction of MOO model based on building ES and emission reduction

The determination of CE indexes is the basis for the MOO study of EC in the operation of EBs. By defining the CE index, it can quantify the CE of EBs in the process of operation, and provide a clear target and evaluation standard for the subsequent optimization study. To establish the CE index of EBs in the operation stage to realize the ES standard, the study firstly launches the prediction of building carbon peak CE factor. The prediction process is shown in Figure 1.

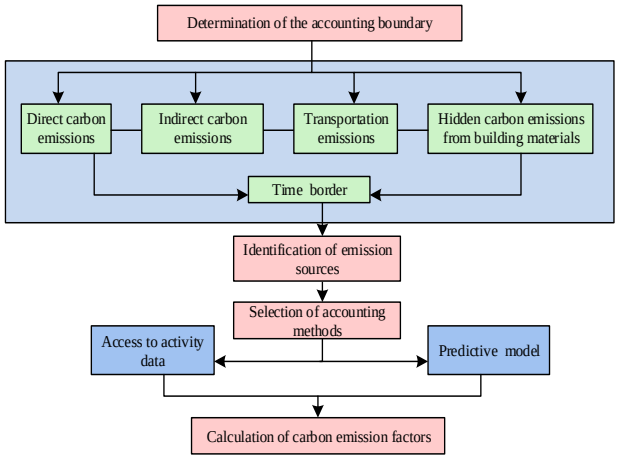

Figure 1: CE accounting process of EBs

As shown in Figure 1, the spatial boundary of the CE calculation is the area of the building and its annexes, and the time boundary is the life cycle of the building. The direct source of CE is the combustion of fuel in buildings, and the calculation factors include fuel type, fuel consumption, and fuel CE factor. Indirect CE refers to the use of electricity and heat, with calculation factors including electricity consumption, CE factors from electricity sources, and CE factors from heat consumption and heat. Transportation emissions refer to the transportation of building materials (BMs) and construction processes, with calculation factors including transportation distance, mode, and CE factors of transportation vehicles. Hidden CE refer to the CE during the production, transportation, and construction processes of BMs. The calculation factors include the type of BMs and the CE factors during the production and transportation stages of the materials. In addition, included are CEs from building-related transportation operations as well as CEs from the choice and application of BMs. With reference to the *Standard for Calculating CEs from Buildings (GB/T51366-2019)*, Equation (1) illustrates how CEs G are calculated during a building's whole life cycle.

$$G = G_s + G_j + G_y + G_c \tag{1}$$

In Equation (1), G_s, G_j, G_y, and G_c represent the emissions ($kgCO_2e/m^2$) from the production of BMs, building construction, operation, and demolition stages,

respectively. The CEs in the building production stage mainly come from the mining, production, transportation, and construction of BMs. Carbon accounting is shown in Equation (2).

$$G_s = \sum AD_i \times EF_i \tag{2}$$

In Equation (2), AD_i denotes the activity volume of the first BM. EF_i is the CE factor of the i th BM, i.e. the CE corresponding to the unit activity volume. Carbon accounting in the operation phase of the building is shown in Equation (3).

$$G_y = \sum P_i \times PF_i \tag{3}$$

In Equation (3), P_i denotes the amount of energy consumed by Type i energy sources. PF_i represents the CE factor of the i th type of energy. The EB retrofit process needs to consider the CEs from operation and retrofit at the same time. The calculation of CE G_g of building retrofit is shown in Equation (4).

$$G_g = G_{gs} + G_{gc} \tag{4}$$

In Equation (4), G_{gs} and G_{gc} represent the CEs caused by the production of BMs and construction in the remodeling process, respectively. Based on the CE accounting of EBs at different stages, the study builds a basic CE factor prediction framework with the help of classical BPNN. BPNN consists of input layer, hidden layer, and output layer (OL). The work signal and the error signal propagate in the BPNN simultaneously. Until the actual output is produced at the output, the work signal continues to travel forward. Layer by layer, the erroneous signal travels backwards from the output. The expression of the error E is shown in Equation (5).

$$E = \frac{1}{2}\sum_{s=1}^{N}\sum_{z=1}^{m}\left(d_{zs}\text{-}y_{zs}\right)^2 \tag{5}$$

In Equation (5), s denotes the data sample. z denotes the input. d and y denote the expectation and prediction of the OL nodes, respectively. To make the output as close to the intended target as possible, the learning objective of BPNN is to adjust its weights based on the error between the network's actual output and the target vector. The updating process of the weight factor SS is shown in Equation (6).

$$\Delta w = w - \alpha\frac{\partial E}{\partial w} \tag{6}$$

In Equation (6), α denotes the hyper-parameter learning rate, which takes the value of 0.01. In addition, BPNN utilizes the chain rule to decompose the gradient of the loss function into local gradients. The simplified computational procedure is shown in Equation (7).

$$\delta_k = -\frac{\partial E}{\partial I_k} = -\frac{\partial E}{\partial y_k}\frac{\partial y_k}{\partial I_k} = (d_k - y_k)f'(I_k) = y_k(1-y_k)(d_k - y_k) \tag{7}$$

In Equation (7), δ_k denotes the error signal. I_k denotes the input of the k th node of the OL. Finally, the study predicts the CE factor when the carbon peaks according to BPNN. The input layer of BPNN receives key feature data that affect the CE factor, including BM parameters, EC data, building structure parameters, and environmental parameters. The hidden layer is used for nonlinear mapping and feature extraction, adopting a single hidden layer structure to avoid overfitting and using the ReLU function to alleviate the gradient vanishing problem. The prediction target of the OL is the CE factor during the building operation phase, with a node count of 1. The activation function is selected as a linear function to directly output continuous values. The core module of the CE prediction framework, known as BPNN, possesses the capability to dynamically modify the CE factor. This modification is contingent upon real-time input EC data and building parameters. BPNN facilitates the iterative solution of multi-objective optimization models. Subsequently, the spatial model of the building is constructed using computer-aided design software according to the construction standards of the EB, and the building model constructed by the study is oriented in the north-south direction with reference to *GB50176-2016 Thermal Design Code for Civil Buildings*. Moreover, it comprehensively considers the building structure and environmental characteristics to determine the transformation parameters, including the transformation of lighting, thermal environment, and envelope structure. Finally, the study synthesizes the CE factor and ES demand at the time of carbon peaking, and determines the CE index of EBs with reference to the *Energy Conservation Design Standard for Public Buildings (GB50189-2015)*.

Energy retrofit of EBs mainly involves windows, lighting, envelope, cooling and heating systems. Window retrofit is an important part of EC retrofit, and the study mainly takes the window-to-ground ratio (WGR) as the retrofit standard. The lighting schematic of the building rooms is shown in Figure 2.

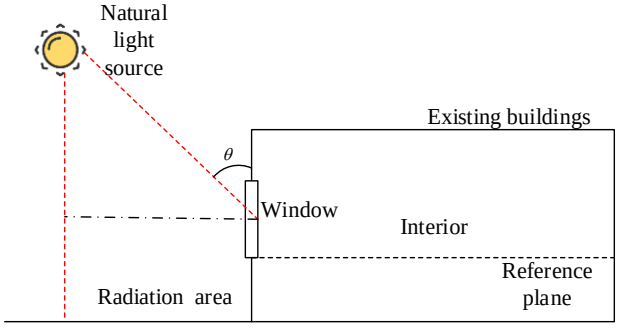

Figure 2: Schematic diagram of room lighting in the EB

In Figure 2, the WGR affects the lighting of the building. The average lighting coefficient C_{av} of a room is calculated in Equation (8).

$$\begin{cases} WGR = \dfrac{A_w}{A_{sum}} \\ C_{av} = \dfrac{A_w \tau\theta}{A_{sum}(1-\rho^2)} \end{cases} \tag{8}$$

In Equation (8), A_w and A_s denote window and room areas, respectively. θ denotes the elevation angle between the window center and the sun. τ denotes the

light transmission ratio. ρ denotes the reflectance ratio. The study uses Ecotect Analysis building simulation software to simulate the change of WGR and lighting coefficient. Supplemental artificial lighting is also required when natural lighting is insufficient. The total indoor illuminance value is composed of the natural lighting illuminance value and the lamp illuminance value. Finally, the final optimal WGR and illuminance values are determined according to the *Building Lighting Design Standard GB50033-2013*, and the number and power of luminaires are then determined. The heat balance of the envelope involves a number of aspects such as building EC, indoor thermal environment, and ES design of the building, and is mainly divided into the envelope modification of non-transparent and transparent envelopes [18-19]. The heat balance process of the two structures is shown in Figure 3.

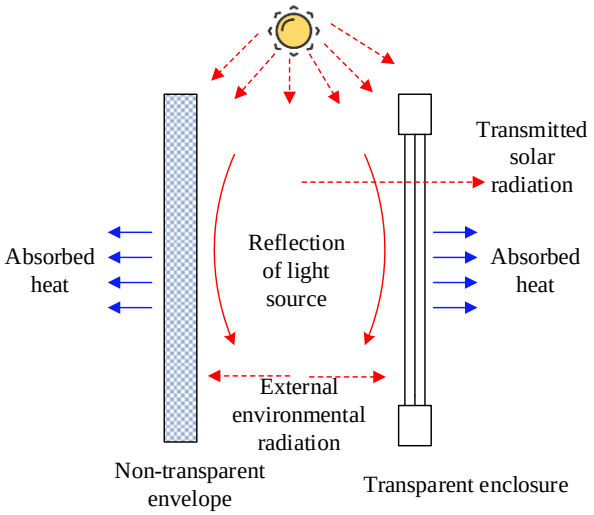

Figure 3: Schematic diagram of the thermal equilibrium of the different structures

In Figure 3, the difference between the two structures is mainly reflected in the fact that the transparent envelope enters a portion of the radiation affecting the heat load of the building. The heat transfer coefficient of the non-transparent enclosure and the indoor-outdoor temperature differential are the primary determinants of the thermal balance. In contrast, the heat balance of the transparent envelope is not only affected by the heat transfer coefficient, but also by the solar heat gain coefficient. In addition, the study introduces the ground source heat pump system to complete the renovation of the cooling and heating system. In summary, the study realizes that the multi-objective of building energy retrofit (BER) is mainly composed of EC and cost. The OF is shown in Equation (9).

$$\begin{cases} f_{\min} = f_{sum}\left(E_{ac}, E_i\right) = f_{ac}(x,K) + f_i(x) \\ g_{\min} = g(x) + g(k) \end{cases} \tag{9}$$

In Equation (9), $f_{\min}$ represents the minimum EC. E_{ac} represents the EC of the air conditioner. E_i represents the EC of lighting. $f_{ac}(x,K)$ represents the OF for optimizing air conditioning EC. $f_i(x)$ represents the OF for optimizing lighting EC. $g_{\min}$ represents the lowest renovation cost. K represents the heat transfer coefficient. x represents the window to ground ratio coefficient. $g(x)$ represents the cost of window renovation. $g(k)$ represents the renovation cost of the enclosure structure. To ensure the feasibility and rationality of the optimization plan, some additional constraints need to be met, as shown in Equation (10).

$$\begin{cases} K_{\min} \le K \le K_{\max} \\ g(x) + g(k) \le C_{budget} \end{cases} \tag{10}$$

In Equation (10), $K_{\min}$ and $K_{\max}$ represent the minimum and maximum values of the heat transfer coefficient. C_{budget} represents the budget.

3.2 Design of EC optimization solution algorithm based on improved MO-ChOA

Following the completion of the EC optimization model design for EBs, the study presents MOOA as a solution to the challenge of balancing several energies retrofit design goals. The EC MOO process proposed by the study is shown in Figure 4.

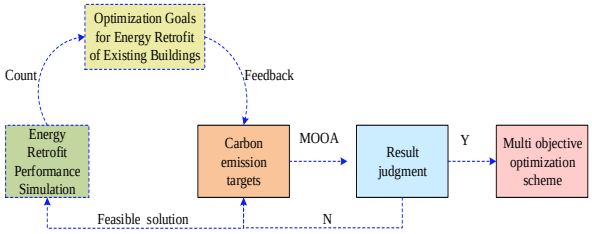

Figure 4: EC MOO process diagram

In Figure 4, the EC optimization process mainly includes three modules: determining the CE index, energy reform performance simulation, and optimization of CE index. The CE index and EC transformation OF are input into MOOA, and the search of the optimal solution is completed by using the CE index to search the solution space. The results of the energy reform performance simulation can be fed back into MOOA again, and the parameters of the algorithm can be adjusted according to the simulation results to complete the optimization of energy reform. The intelligent optimization algorithm used in the study is ChOA. ChOA is an intelligent optimization algorithm based on chimpanzee population behavior, which is characterized by fast convergence speed and high computational accuracy. ChOA mimics the strategies and behaviors of chimpanzee populations in terms of hunting, communication, and decision-making. It categorizes the population into attackers, interceptors, repellers and chasers. Attacking chimpanzees are responsible for the final attack behavior, usually representing the optimal solution, and their position vectors (PVs) are used to guide other chimpanzees to update their positions. The pursuers are responsible for collaborating with the repelling chimpanzees to bring them into attack range, guiding the search process towards the area of potential optimal solutions. Interceptor chimpanzees are responsible for blocking the escape route of prey and assisting other chimpanzees to surround the

prey during the hunting process [20-21]. In the ChOA, the chimpanzee's PV represents the solution vector, and the update process of the PV is also the optimization process of the solution vector. ChOA first randomly generates a certain number of solution vectors to model the initial state of the chimpanzee population and randomly updates the population position. As demonstrated by Equation (11), during the exploration phase, population members adjust their positions in accordance with the prey's position.

$$\begin{cases} X_{chimp}^{t+1} = X_{prey}^{t} - a \cdot d \\ d = \left| c \cdot X_{prey}^{t} - m \cdot X_{chimp}^{t} \right| \end{cases} \tag{11}$$

In Equation (11), X_{prey}^{t} represents the PV of the prey at time t. X_{chimp}^{t} and X_{chimp}^{t+1} represent the PV of individuals in the population at time t and time $t+1$, respectively. a denotes the coefficient vector, which is controlled by the convergence factor. d denotes the distance between the prey and the population. c denotes the influence factor of obstacles on the prey of the population. m denotes the chaotic mapping vector. During the exploitation phase, the chimpanzee population approaches the optimal solution by collaboratively updating their positions, which are shown in Equation (12).

$$X^{t+1} = \frac{X_1^{t+1} + X_2^{t+1} + X_3^{t+1} + X_4^{t+1}}{4} \tag{12}$$

In Equation (12), X_1^{t+1}, X_2^{t+1}, X_3^{t+1}, and X_4^{t+1} denote the updated PVs of the attacker, encircler, repeller, and pursuer, respectively. However, the initial population generation of traditional ChOA is too random, which leads to poor diversity and uniformity of the population distribution of the algorithm and affects the algorithm's traversal of the solution space [22-23]. In this regard, the study introduces the Hammersley sequence to help ChOA generate the initial population. The Hammersley sequence can generate a uniformly distributed point set in the multidimensional space. The improved calculation of the initial position of the population is shown in Equation (13).

$$X_k = l_b + H_k (u_b - l_b) \tag{13}$$

In Equation (13), u_b and l_b denote the upper and lower bounds of the positional variable interval. H_k denotes the Hammersley sequence. The Hammersley sequence is a low variance sequence that can generate uniformly distributed sample points. In ChOA, the Hammersley sequence first determines the number and dimension of the sample points. Second, the first d-1 primes are selected to generate Halton sequences in other dimensions. Then, Hammersley sequences are generated and the sequences for each dimension are combined to form complete Hammersley sequential sampling points. Finally, the sampling points are normalized to map them to actual variable ranges. Moreover, the generated sample points are used as the initial totality for the optimization of the algorithm. In addition, the traditional ChOA is prone to gradual convergence of population individuals to the local optimal solution as the number of iterations increases, resulting in the algorithm's difficulty in jumping out of this local optimal region. In this regard, the study introduces the somersault foraging heuristic strategy, which simulates the behavior of an animal looking for more food by somersaulting during foraging. The working mechanism is shown in Figure 5.

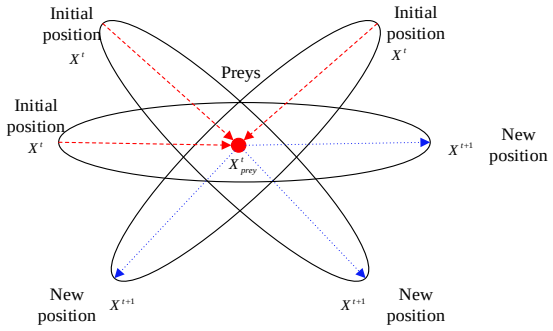

Figure 5: Mechanism of the somersault foraging heuristic working mechanism

As demonstrated in Figure 5, the somersault foraging strategy emulates the foraging behavior of organisms and updates the current solution symmetrically to the opposite side of the fulcrum. This allows the algorithm to explore the symmetric region of the current position, thereby increasing the diversity of the search and avoiding premature convergence of the population to the local optimal solution. In addition, the random number of the somersault foraging strategy also introduces randomness into the update process, making it possible to generate different new solutions with each update. The mathematical expression is given in Equation (14).

$$X^{t+1} = X^{t} + S(r_1 \cdot X_{prey}^{t} - r_2 \cdot X^{t}), if \quad i/N > r, r \in [0,1] \tag{14}$$

In Equation (14), S is the blanking factor. r denotes the random number. N is the maximum iterations' quantity. Finally, the study draws on NSGA II to design a multi-objective search strategy for improving ChOA, which mainly includes fast non-dominated sorting, congestion comparison operator, and elite strategy. The working mechanism is shown in Figure 6.

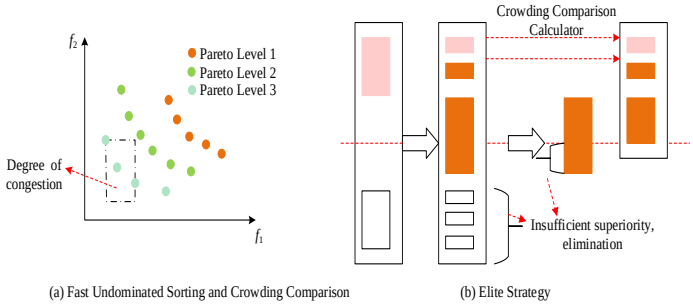

Figure 6: Multi-objective search strategy of improved MO-ChOA

In Figure 6, based on the population's fitness and each person's Pareto dominance connection, the enhanced MO-ChOA first completes the population hierarchy. Then, the comparison of individuals between the same tiers is performed. Finally, the optimal solution of the previous generation is retained and the multi-objective search is performed again for the new population of the next generation. The complexity analysis of the improved MO-CHOA is performed. It is assumed that the population size is N and the dimensionality of the decision variables is D. The computational complexity of the improved MO-CHOA to generate the initial population and the somersault foraging strategy is O(N·D). It is assumed that the computational complexity of the fitness function is O(F), and the complexity of each fitness computation is 0(N·F). The computational complexity of fast non-dominated sorting is $O(M \cdot N^2)$, where M represents the number of targets. The computational complexity of the crowding comparison operator is O(N·logN), and the computational complexity of the elite strategy is O(N·D). It is assumed the algorithm runs T iterations, the overall complexity of the improved MO-CHOA is $O[T(M \cdot N^2+N \cdot F+N \cdot \log N+N \cdot D)$.

4 Building energy retrofit MOOA performance testing and application effect analysis

To verify the effectiveness of the research-designed MOO model for BER and the improved MO-ChOA, the research launched performance testing and application analysis experiments.

4.1 MOOA performance testing

The comparative analysis of MOOA is unfolded first. The experiment is completed based on Windows 10 operating system; the central processor is Intel(R) Core (TM) i5-6300HQ with 16G of RAM. The image processor is GTX 3060 12G. The algorithm implementation language is Python3.8. Using hyper volume (HV) and inverse generation distance (IGD) as evaluation metrics. HV is employed to assess the extent to which the target space is encompassed by an approximate set. A higher value of HV signifies a more comprehensive coverage of the target space by the solution set, thereby indicating a higher quality of the solution. IGD measures the average distance from a reference point set to a solution set, with smaller values indicating that the solution set is closer to the true Pareto front and more evenly distributed. Sensitivity analysis is performed on the ZDT3 function by setting the maximum number of iterations to 100. The population size is set to 50, 100, and 150. The flip factor is set to 1, 3, and 5. The mutation probability is set to 0.01, 0.05, and 0.1, respectively. The results of the hyper-parameter sensitivity analysis of the improved MO-ChOA are shown in Table 2. In this table, a population size too small (50) leads to insufficient diversity and low HV, while a population size too large (150) increases the computational cost and slows down the convergence speed. When the population size is 100, convergence and diversity are balanced. If the flip factor is too small (1), the local search ability of the algorithm is weak, and if it is too large (5), it can lead to oscillations. If the mutation probability is too low (0.01), the algorithm will tend to get stuck in local optima. Furthermore, if it is too high (0.1), it will lead to a decrease in the convergence performance of the algorithm. When the population size is 100, the flip factor is 3, and the mutation probability is 0.05. Moreover, the improved MO-ChOA performs best in HV and IGD indicators, with values of 0.973 and 0.113, respectively. Therefore, in the study, the population size is set to 100, the flip factor is set to 3, and the mutation probability is set to 0.05.

Table 2: Hyper-parameter sensitivity analysis results

Hyper-parameters		HV	IGD
Population size	50	0.952	0.125
	100	0.973	0.113
	150	0.962	0.119
Flip factor	1	0.931	0.142
	3	0.973	0.113
	5	0.958	0.121
Mutation probability	0.01	0.962	0.129
	0.05	0.973	0.113
	0.10	0.955	0.124

The test functions include the dual-OF ZDT3, and the triple-OFs are DTLZ1 and DTLZ3. ZDT3 is a dual objective optimization test function with one global optimal solution and multiple local optimal solutions, which is commonly used to test the global convergence ability and local optimal solution avoidance ability of algorithms. DTLZ1 and DTLZ3 are multi-objective optimization test functions commonly used to test the performance of algorithms in multi-objective optimization problems. The performance of MO-CHOA on the test function before and after improvement is shown in Figure 7. Comparing Figure 7 (a) and (b), the improved MO-ChOA has a better solution on the ZDT3 function, and the solution value is more uniformly fit to the real frontier. The traditional MO-ChOA has poorer convergence of the solved values with more breakpoints. Comparing Figures 7(c) and (d), the improved MO-ChOA has better convergence on the DTLZ1 function, and the solved values are uniformly distributed on the frontiers, which can cover the true frontiers better. The solution deviation of the traditional MO-ChOA is obviously increased. Comparing with Figures 7(e) and (f), the improved MO-ChOA has better distributability on the DTLZ3 function, the overlap of the solution set gets reduced, the blank region of the true frontier is reduced, and the solution set distributability is superior. The results indicate that the improved MO-ChOA proposed by the study has a better multi-objective solution performance compared to the MO-ChOA. This is because the improved MO-ChOA uses a uniform initial population generated by Hammersley sequences, which can explore the search space more widely and avoid getting stuck in local optima. Meanwhile, the somersault foraging strategy further enhances the global search capability of the algorithm,

enabling it to more accurately find the global optimal solution. In addition, the multi-objective search strategy of NSGA II ensures the diversity and convergence of the solution, so that the solution values of the algorithm more closely match the real frontier. However, traditional MO-ChOA lacks these enhancements, resulting in poor convergence, multiple breakpoints, and poor distribution of the solution set.

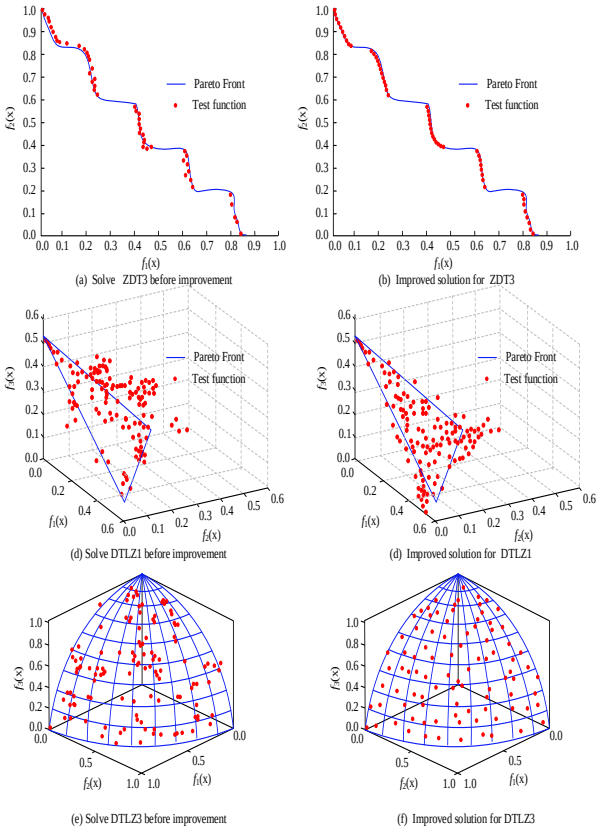

Figure 7: Performance of MO-ChOA on test functions before and after improvement

To verify the effectiveness of the proposed improvement strategy, ablation experiments are performed on the ZDT3 function. The original MO-ChOA, MO-ChOA with Hammersley sequences only, MO-ChOA with somersault foraging heuristic strategy only, MO-ChOA with NSGA II multi-objective search strategy only, and the complete algorithm are compared. The results of the ablation experiment are shown in Table 3. The full model performs best in terms of HV and IGD indicators. Next is the MO-ChOA, which only introduces the NSGA II multi-objective search strategy, with HV and IGD indicators of 0.765 ± 0.020 and 0.121 ± 0.008, respectively. This indicates that the NSGA II multi-objective search strategy contributes the most to improving the performance of MO-CHOA.

Table 3: Results of ablation experiment

Algorithm	HV	IGD
MO-ChOA	0.674±0.012	0.150±0.014
Hammersley+MO-ChOA	0.742±0.018	0.129±0.009
Heuristic strategy of somersault for foraging+MO-ChOA	0.721±0.015	0.134±0.012
NSGA II+MO-ChOA	0.765±0.020	0.121±0.008
Improved MO-CHOA	0.973±0.009	0.113±0.005

Compared with traditional MO-CHOA, MOPSO, non-dominated sorting genetic algorithm III (NSGA-III), and MOEA in reference [16]. The MOPSO algorithm simulates the foraging behavior of flocks of birds, finds the optimal solution through cooperation and competition among particles. Moreover, it introduces diversity search strategy and convergence search strategy to enhance the diversity and convergence of solutions. NSGA-III is a multi-objective algorithm based on evolutionary optimization, which uses genetic operations to optimize multiple conflicting objectives. Furthermore, it employs non-dominant sorting and crowding distance mechanisms to maintain population diversity and quality. MOEA is an algorithm that solves multi-objective optimization problems by simulating the process of biological evolution to simultaneously optimize multiple conflicting objectives. It uses dominance-based relationships and diversity preservation mechanisms to generate Pareto optimal solution sets. The comparison results of HV and IGD values for different algorithms are shown in Figure 8. In Figure 8(a), the IGD curve of the improved MO-ChOA is always at the lowest level, and the minimum value converges to 0.113, which is the closest distance to the real frontier, in line with the solution distribution in Figure 7. In contrast, the IGD values of the conventional MO-ChOA, MOPSO, NSGA-III, and MOEA converge at 0.353, 0.341, 0.301, and 0.295, respectively. Hammersley sequences with heuristic strategies to improve the convergence of the solution set. In Figure 8(b), the HV curve of the improved MO-ChOA grows the fastest and quickly converges to 0.973 at the late stage of iteration. The IGD values of the traditional MO-ChOA, MOPSO, NSGA-III, and MOEA converge to 0.826, 0.768, 0.751, and 0.820, respectively. The improved approach raises the convergence and diversity of the solution set while also improving the algorithm's overall performance.

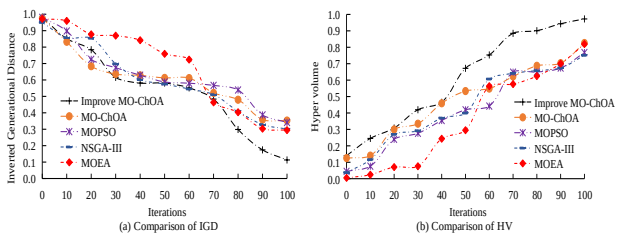

Figure 8: Comparison of HV and IGD values for different algorithms

The study used binary metrics (coverage metric, C-Metric) and knee driven dissimilarity (KD) as evaluation indicators. C-Metric is a performance metric used to measure the dominance relationship between two solution sets. It can evaluate which algorithm generates a solution set with better dominance relationship. KD is mainly used to measure the difference between the solution set and the

true knee point. The smaller its value, the closer the solution set is to the true knee point, and the better the algorithm performance. Adding more test functions to compare the different algorithms for solution set solving quality, Figure 9 displays the outcomes of the experiment. In Figure 9(a) and (b), the improved MO-ChOA designed by the study achieves the maximum C-metric on the test function ZDT3, which takes the value of 0.991. The C-metric is used to measure the degree of superiority of one solution set with respect to another solution set. That is, what percentage of solutions in one solution set is dominated by a particular solution in another solution set. Meanwhile, the minimum value of KD of 0.118 is obtained on the SCH test function. In Figure 9(c) and (d), the C-metric and KD values of other MOOA are worse than those of the improved MO-ChOA. The solution set of the algorithm can cover the real solution set more widely.

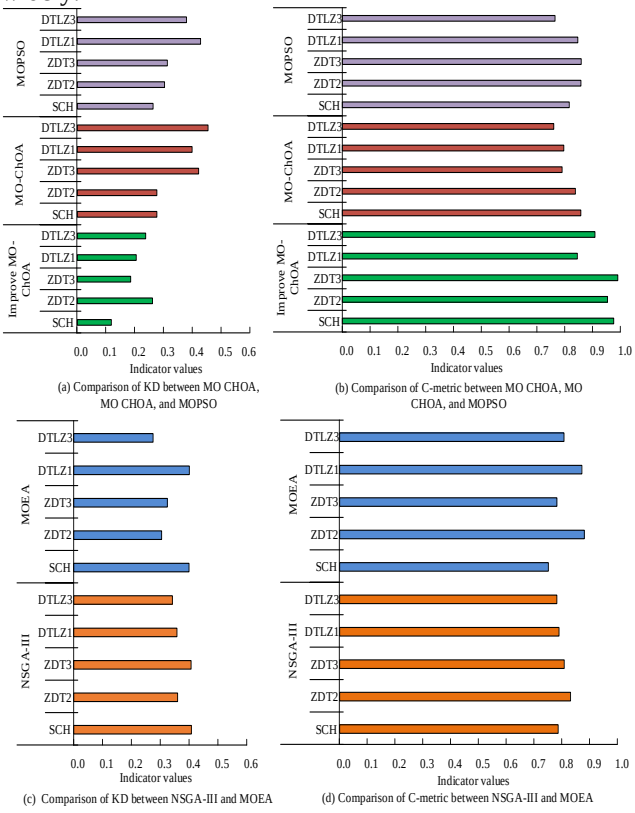

Figure 9: Comparison of C-metric and KD values for different algorithms

4.2 Effect of the application of building EC optimization

To verify the practical application effect of the proposed improved MO-ChOA, this study takes an EB in a city in China as an example to carry out EC optimization and renovation. The building is constructed in the 1990s, with a total area of about 5000 square meters and an annual CE target of 2.81 kg CO_2e/m^2. The energy utilization efficiency is relatively low, mainly relying on traditional central heating and air conditioning systems. The annual EC for cooling and heating is 27.81 kW·h/m^2, lighting EC is 6.95 kW·h/m^2, and other EC is 3.86 kW·h/m^2. The heat transfer coefficients of the interior and exterior walls of the building are 1.52W/(m^2 · k) and 0.92W/(m^2 · k), respectively. The heat transfer coefficient of the windows is 2.9W/(m^2·k), and the heat transfer coefficient of the doors is 1.35W/(m^2·k). A comprehensive optimization of the building's heating, air conditioning, lighting, and building envelope is planned. The solution quality of different algorithms in energy optimization is shown in Figure 10. In Figure 10(a), there is a significant difference in the solution spacing performance (SP) of different algorithms. Improved MO-ChOA has the smallest range of SP distribution. During 120 iterations, the minimum SP value is only 0.110. It can be concluded that the solutions inside the Pareto solution set of Improved MO-ChOA are denser and more diverse. While the minimum SP values of the other algorithms are on the level of 0.20 values. In Figure 10(b), the improved MO-ChOA performs well in uniformity performance (UP), with the average UP values all above the 0.80 taking level. Taken together, the studied design achieves the most widely distributed solution set in energy optimization.

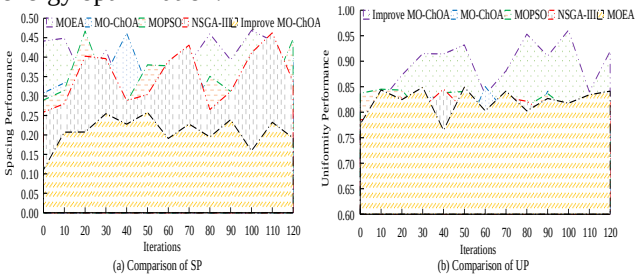

Figure 10: Comparison of SP and UP for different algorithms

The ESs rate (ESR) and CE savings ratio (CESR) of the building are compared after optimization with different algorithms. Figure 11 displays the outcomes of the experiment. Following energy optimization, the optimization scheme produced by the upgraded MO-ChOA in Figure 11(a) produces the maximum ESR fetch while the building is in operation. It is substantially superior to the solution schemes of other algorithms, fluctuating between 0.8 and 1.0. Following the building's refurbishment, the higher ESR readings indicate a notable decrease in EC and an increase in energy use efficiency. The retrofit effect of the other solutions is not significant and the reduction of EC is limited. In Figure 11(b), the optimization scheme obtained by the improved MO-ChOA obtained the highest CESR fetch value, fluctuating within the interval of 0.7-0.95. The method effectively reduces the carbon footprint of the building with less negative impact on the environment. China's *Energy Consumption Standards for Civil Buildings* has set binding and guiding indicators for building EC, and the energy-saving rate of the *Energy Efficiency Design Standards for Public Buildings* has increased from 65% to 72%. The improved MO-ChOA proposed in this study optimized the ESR of the building within the range of 0.8-1.0, which is much higher than the energy-saving rate

level of the energy-saving benchmark building. This indicates that the EC of the renovated building has been significantly reduced and the energy utilization efficiency has been improved, reaching the leading energy-saving level in China.

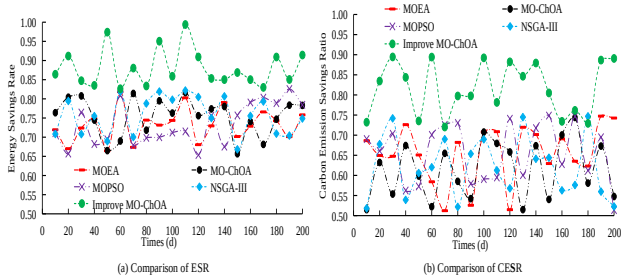

Figure 11: Comparison of ESR and CESR for different algorithms

The results of cost savings ratio (CSR) and return on investment (ROI) obtained by different algorithmic optimization schemes are shown in Figure 12. In Figure 12(a), the CSR curve of the improved MO-ChOA is the highest throughout the iterative optimization process, converging to the highest value of 0.790. It demonstrates that by increasing energy efficiency and lowering EC, the energy optimization plan lowers energy bills and other associated expenses. In Figure 12(b), the ROI of the Improved MO-ChOA is the highest, taking the value of 0.685. In summary, the scheme has significantly reduced the operating costs of the retrofitted building, with a high ROI and a high economic feasibility of the project.

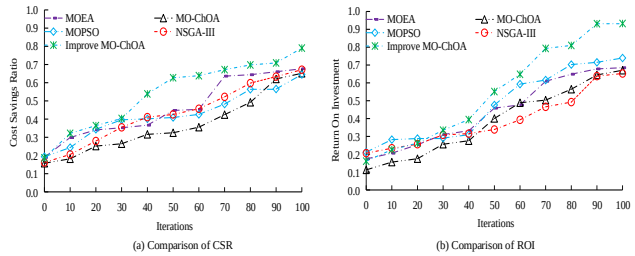

Figure 12: Comparison of CSR and ROI of different algorithms

5 Discussion

To optimize the operational EC of EBs, an improved MO-ChOA was proposed. The results showed that the convergence of the solution value of the improved MO-ChOA was better and could cover the real frontier better. The minimum value of IGD converged to 0.113 and the maximum value of HV converged to 0.973. IGD reflected the degree of closeness between the solution set and the true frontier, while HV was used to measure the coverage and overall quality of the solution set. The improved MO-ChOA focused more on the convergence of the solution set rather than the coverage area. Therefore, IGD had been significantly improved, but HV remained similar. The C-metric value of the improved MO-ChOA could reach 0.991 on the ZDT3 test function, and the KD value was only 0.118 on the SCH test function. Meanwhile, the minimum value of SP was only 0.110, and the UP values were all at the 0.80 fetch level. The investigated design achieved the most widely distributed solution set in energy optimization. During the operation of the building after energy optimization, the optimized solution obtained by improving MO-ChOA achieved the best ES rate and economic feasibility. The ESR took values fluctuating in the range of 0.8-1.0, the CESR took values fluctuating in the range of 0.7-0.95, the CSR converged to the highest value of 0.790, and the ROI took values as high as 0.685. The ESR, CESR, CSR, and ROI were all higher than the MOEA algorithm, indicating that the application effect was better than the MOEA algorithm proposed by Khan et al. [16]. In addition, the HV index of the method proposed by Zhao et al. [14] was 0.891, and the IGD index was 0.201. The HV index of the method proposed by Wei et al. [17] was 0.902 and the IGD index was 0.148, both of which performed worse than the algorithm in this study. It can be concluded that the improved MO-ChOA proposed by the research had a good multi-objective optimization performance. This was because the Hammersley sequence and the somersault strategy introduced in the study could generate an initial population by multi-dimensional uniform distribution. Moreover, the step size was controlled by the flip factor to make the algorithm jump out of local optima. The NSGA-II multi-objective search strategy could balance convergence and distribution. Compared to traditional MO-ChOA and NSGA-II algorithms, it was closer to the real frontier.

The proposed method can significantly reduce the EC of buildings during operation, thereby increasing the economic value and market competitiveness of buildings. Although in the case analysis, this study focuses on a specific building in a Chinese city and may not directly reflect the actual operation of other buildings. However, the proposed improved MO-ChOA has universality in principle and good scalability under different building types and climatic conditions. It can be combined with the automation control system of industrial buildings to optimize and schedule EC in the production process. To further improve the adaptability of the proposed method in different building types and climates, the optimization objectives and constraints can be redefined or adjusted.

In addition, the optimization and renovation of building EC also face various limitations in practical situations. In terms of data reliability, the collection of building EC data relies on various sensors and metering devices that may experience malfunctions or errors, resulting in inaccurate or incomplete data collection. In building renovation, the fact that the building is already in use and the construction space is limited, some large construction equipment cannot enter the site, which limits the choice of construction techniques and methods. Moreover, some EBs may have structural safety hazards due to their long construction history. To address the above issues, cross-validation and correction of anomalous data can be achieved by combining information from multiple data sources, such as fusing meter data with power sensor data to improve data accuracy and reliability. Prior to the initiation of construction renovations, a comprehensive survey of the building site should be conducted to formulate a

scientifically sound construction plan, methodically arrange the construction process, and develop appropriate reinforcement and repair strategies for addressing structural safety hazards.

6 Conclusion

To find the optimal retrofit solution through the optimization algorithm in the retrofit of EBs by simultaneously considering multiple objectives such as ES, economy, and comfort, the study implemented the solution of EC MOOA based on the improved MO-ChOA. The study provides effective technical means for the ES retrofit of EBs and promotes the development of the construction industry in the direction of low-carbon and sustainable development. However, the design of the study does not take into account the differences in structure, function, and usage patterns of different buildings, and the applicability of improving MO-ChOA needs to be further explored.

References

[1] Xue Q, Wang Z, Chen Q. Multi-objective optimization of building design for life cycle cost and CO2 emissions: A case study of a low-energy residential building in a severe cold climate. Building simulation. Building simulation, 2022, 15(1): 83-98, doi: 10.31449/inf.v49i16.7705.

[2] Khafaga D S, El-kenawy E S M, Alhussan A A, Eid M M. Forecasting energy consumption using a novel hybrid dipper throated optimization and stochastic fractal search algorithm. Intelligent Automation & Soft Computing, 2023, 37(2): 2117-2132, doi: 10.32604/iasc.2023.038811.

[3] Erebor EM, Ibem EO, Ezema IC, Sholanke A B. Building Professional Practices Knowledge and Integration Levels of Energy Efficiency Design Features in Selected Office Buildings in Abuja, Nigeria. Environment and Ecology Research, 2022, 10(3): 414-426, doi: DOI:10.13189/eer.2022.100309.

[4] Zhang T, Yang X. Energy-Saving Design of Smart City Buildings Based on Deep Learning Algorithms and Remote Sensing Image Scenes. Informatica, 2024, 48(19): 103-118, doi: 10.31449/inf.v48i19.6049.

[5] Fang Q, Zhang J, Xu Z, Lv Y, Pi J. Construction of Sustainable Building Performance Optimization Design Model Based on Sensitive Multi-Objective Decision Making. Informatica, 2024, 48(13): 81-96, doi: 10.31449/inf.v48i13.6013.

[6] Fallah A M, Ghafourian E, Shahzamani Sichani L, Ghafourian H, Arandian B, Nehdi M L. Novel neural network optimized by electrostatic discharge algorithm for modification of buildings energy performance. Sustainability, 2023, 15(4): 2884-2898, doi: 10.3390/su15042884.

[7] Tahmasebinia F, Lin L, Wu S, et al. Exploring the benefits and limitations of digital twin technology in building energy. Applied Sciences, 2023, 13(15): 8814-8851, doi: 10.3390/app13158814.

[8] Verma A, Prakash S, Kumar A. AI-based building management and information system with multi-agent topology for an energy-efficient building: towards occupant's comfort. IETE Journal of Research, 2023, 69(2): 1033-1044, doi: 10.1080/03772063.2020.1847701.

[9] Sana A F, Dibakar R, Bishwajit B. Genetic Algorithm and Grasshopper Optimization Algorithm with Metaoptimization and RL-Based Parameter Fine-Tuning and Their Comparison for Optimal Thermal Performance Analysis of Buildings in Tropical Climate. Journal of Computing in Civil Engineering, 2025, 39(2): 164-186, doi: 0.1061/JCCEE5.CPENG-6159.

[10] Wu Y. Design and analysis of energy efficient urban buildings based on BIM model. Journal of Computational Methods in Sciences and Engineering, 2024, 24(6): 3785-3798, doi: 10.1177/14727978241296348

[11] Khan F A, Ullah K, ur Rahman A, Anwar S. Energy optimization in smart urban buildings using bio-inspired ant colony optimization. Soft Computing, 2023, 27(2): 973-989, doi: 10.1007/s00500-022-07537-3.

[12] Xu F, Liu Q. Building energy consumption optimization method based on convolutional neural network and BIM. Alexandria Engineering Journal, 2023, 77(6): 407-417, doi: 10.1016/j.aej.2023.06.084.

[13] Gheouany S, Ouadi H, El Bakali S. Hybrid-integer algorithm for a multi-objective optimal home energy management system. Clean Energy, 2023, 7(2): 375-388, doi: 10.1093/ce/zkac082.

[14] Zhao N, Zhang J, Dong Y, Ding C. Multi-Objective Optimization and Sensitivity Analysis of Building Envelopes and Solar Panels Using Intelligent Algorithms. Buildings, 2024, 14(10): 3134-3151, doi: 10.3390/buildings14103134.

[15] Ding Z, Li J, Wang Z, Xiong Z. Multi-Objective Optimization of Building Envelope Retrofits Considering Future Climate Scenarios: An Integrated Approach Using Machine Learning and Climate Models Sustainability, 2024, 16(18): 8217-8233, doi: 10.3390/su16188217.

[16] Khan A M, Tariq M A, Rehman S K U, Saeed T, Alqahtani F K, Sherif M. BIM integration with XAI using LIME and MOO for automated green building energy performance analysis. Energies, 2024, 17(13): 3295-3316, doi: 10.3390/en17133295.

[17] Wei H, Jiao Y, Wang Z, Wang W, Zhang T. Optimal retrofitting scenarios of multi-objective energy-efficient historic building under different national goals integrating energy simulation, reduced order modelling and NSGA-II algorithm. Building Simulation. Tsinghua University Press, 2024, 17(6): 933-954, doi: 10.1007/s12273-024-1122-9.

[18] Teng J, Yin H. Carbon emission reduction in public buildings of extreme cold regions: A study on enclosure structure and HVAC system parameter optimization. Energy Science & Engineering, 2024, 12(6): 2676-2686, doi: 10.1002/ese3.1779.

[19] Alelwani R, Ahmad W M, Rezgui Y, Alshammari K. Optimising Energy Efficiency and Daylighting Performance for Designing Vernacular Architecture—A Case Study of Rawshan. Sustainability, 2025, 17(1): 315-315, doi: 10.3390/su17010315.

[20] Daoud M S, Shehab M, Abualigah L, Alshinwan, M., Elaziz M A, Shambour M K Y, Zitar R. A. Recent Advances of Chimp Optimization Algorithm: Variants and Applications. Journal of Bionic Engineering, 2023, 20(6): 2840-2862, doi: 10.1007/s42235-023-00427-w.

[21] Khishe M. Greedy opposition-based learning for chimp optimization algorithm. Artificial Intelligence Review, 2023, 56(8): 7633-7663, doi: 10.1007/s10462-022-10343-w.

[22] Qian L, Khishe M, Huang Y, Mirjalili, S. SEB-ChOA: an improved chimp optimization algorithm using spiral exploitation behavior. Neural Computing and Applications, 2024, 36(9): 4763-4786, doi: 10.1007/s00521-023-09236-y.

[23]Usman A M, Abdullah M K. An Assessment of Building Energy Consumption Characteristics Using Analytical Energy and Carbon Footprint Assessment Model. Green and Low-Carbon Economy, 2023, 1(1): 28-40, doi: 10.47852/bonviewGLCE3202545.